Rome's urban history inferred from Pb-contaminated waters trapped in its ancient harbor basins

Hugo Delile, Duncan Keenan-Jones, Janne Blichert-Toft, Jean-Philippe Goiran, Florent Arnaud-Godet, Francis Albarède

Rome's urban history inferred from Pb-contaminated waters trapped in its ancient harbor basins

Hugo Delile[a,b,c,1], Duncan Keenan-Jones[d], Janne Blichert-Toft[c], Jean-Philippe Goiran[a], Florent Arnaud-Godet[c], and Francis Albarède[c]

[a]Maison de l'Orient et de la Méditerranée, CNRS UMR 5133, 69365 Lyon Cedex 7, France; [b]Department of Archaeology, University of Southampton, Southampton SO17 1BF, United Kingdom; [c]Ecole Normale Supérieure de Lyon, Université Claude Bernard-Lyon I, CNRS UMR 5276, 69007 Lyon, France; and [d]Classics, School of Humanities, University of Glasgow, Glasgow, Lanarkshire G12 8QQ, United Kingdom

Edited by Jeremy A. Sabloff, Santa Fe Institute, Santa Fe, NM, and approved July 12, 2017 (received for review April 17, 2017)

Heavy metals from urban runoff preserved in sedimentary deposits record long-term economic and industrial development via the expansion and contraction of a city's infrastructure. Lead concentrations and isotopic compositions measured in the sediments of the harbor of Ostia—Rome's first harbor—show that lead pipes used in the water supply networks of Rome and Ostia were the only source of radiogenic Pb, which, in geologically young central Italy, is the hallmark of urban pollution. High-resolution geochemical, isotopic, and ^{14}C analyses of a sedimentary core from Ostia harbor have allowed us to date the commissioning of Rome's lead pipe water distribution system to around the second century BC, considerably later than Rome's first aqueduct built in the late fourth century BC. Even more significantly, the isotopic record of Pb pollution proves to be an unparalleled proxy for tracking the urban development of ancient Rome over more than a millennium, providing a semiquantitative record of the water system's initial expansion, its later neglect, probably during the civil wars of the first century BC, and its peaking in extent during the relative stability of the early high Imperial period. This core record fills the gap in the system's history before the appearance of more detailed literary and inscriptional evidence from the late first century BC onward. It also preserves evidence of the changes in the dynamics of the Tiber River that accompanied the construction of Rome's artificial port, *Portus*, during the first and second centuries AD.

paleopollution | lead pipes | Pb isotopes | harbor geoarcheology | Ostia

Recent cases of lead contamination of drinking water in the Midwestern United States have highlighted the sensitive equilibrium between essential urban water supply, hydraulic infrastructures, and economic and public health (1). Lead pollution was already affecting the urban waters of great Roman cities two millennia ago (2–4), although to a lesser extent than suggested earlier (2, 5). Harbor sediment cores provide one of the best continuous records of human impact on the local environment. By combining isotopic analysis of lead in harbor sediments with evidence derived from archeological materials (e.g., lead pipes) and carbonates—known as travertine or sinter taken from aqueduct channels—recent studies have shown that the proportion of foreign lead in sediments constitutes a proxy for the expansion and contraction of the water supply system and therefore, of urban development over the lifetime of a city (2–4). Urban centers were particularly vulnerable to the interruption of their water supply network because of natural or human causes (6). Hiatuses in the imported Pb isotopic record of the Trajanic basin sediments at *Portus* (core TR14 in Fig. S1*A*), the maritime port of Imperial Rome, and those from the channel connecting *Portus* with the Tiber (*Canale Romano*) (core CN1 in Fig. S1*A*) reflect the sixth century AD Gothic Wars and ninth century Arab sack of Rome (2). The chronological record at *Portus*, however, only started with Trajan (AD 98–117), leaving the earlier history of Rome's urbanization essentially undocumented, except for sparse archeological evidence and passing mentions in politically biased historical accounts. The same is the case for the development of Rome's water distribution network before the reforms of Agrippa in the late first century BC (6), from which point on the admittedly problematic texts of Vitruvius (7) and Frontinus (Rome's water commissioner century AD 100) (8) provide more information. The first Roman aqueduct, the Aqua Appia (late fourth century BC) (6, 9), appears well before any evidence of widespread use of lead water pipes (*fistulae*; in the late first century BC) (10), raising the question of how water was distributed.

To explore these questions, we conducted a high-resolution analysis of major and trace element concentrations and Pb isotopic compositions of a 12-m-long sediment core (PO2 in Fig. S1 *A* and *B*) from Ostia. Ostia, today a featureless coastal plain near the Tiber River (Fig. S1*B*), was the first harbor to serve Rome (11). The time span encompassed by core PO2 is constrained by 15 radiocarbon dates covering the first millennium BC (Table S1) (12). Lead concentrations and isotopic compositions also were measured on sediments from the PTXI-3 core drilled at *Portus* in the basin of Claudius (AD 41–54) (Fig. S1*A*), the entry port of the Trajan basin, although at a coarser resolution than the PO2 core.

Results

Stratigraphy. The stratigraphy of the PO2 core can be subdivided into three main sedimentary units: preharbor (unit A), harbor (unit B), and postharbor (unit C) (Fig. 1). (*i*) Unit A is represented by bedded and shelly gray sands with *Posidonia*, attesting to a depositional environment of deltaic progradation up to the middle of the fourth century BC (12). (*ii*) Unit B is further subdivided into two subunits, B1 and B2. Subunit B1 forms the lower harbor sequence characterized by compact dark gray silt suggestive of a quiet environment and lasting until the beginning

Significance

Isotopic evidence showing that Rome's lead water pipes were the primary source of lead pollution in the city's runoff reveals the sedimentary profile of lead pollution in the harbor at Ostia to be a sensitive record of the growth of Rome's water distribution system and hence, of the city itself. The introduction of this lead pipe network can now be dated to around the second century BC, testifying to a delay of about a century and a half between the introduction of Rome's aqueduct system and the installation of a piped grid. The diachronic evolution of anthropogenic lead contamination is able to capture the main stages of ancient Rome's urbanization until its peak during the early high empire.

Author contributions: H.D. and J.-P.G. designed research; H.D. and J.B.-T. performed research; F.A.-G. contributed reagents/analytic tools; H.D., D.K.-J., J.B.-T., J.-P.G., and F.A. analyzed data; and H.D., D.K.-J., J.B.-T., and F.A. wrote the paper.

The authors declare no conflict of interest.

This article is a PNAS Direct Submission.

[1]To whom correspondence should be addressed. Email: hugo.delile@mom.fr.

This article contains supporting information online at www.pnas.org/lookup/suppl/doi:10.1073/pnas.1706334114/-/DCSupplemental.

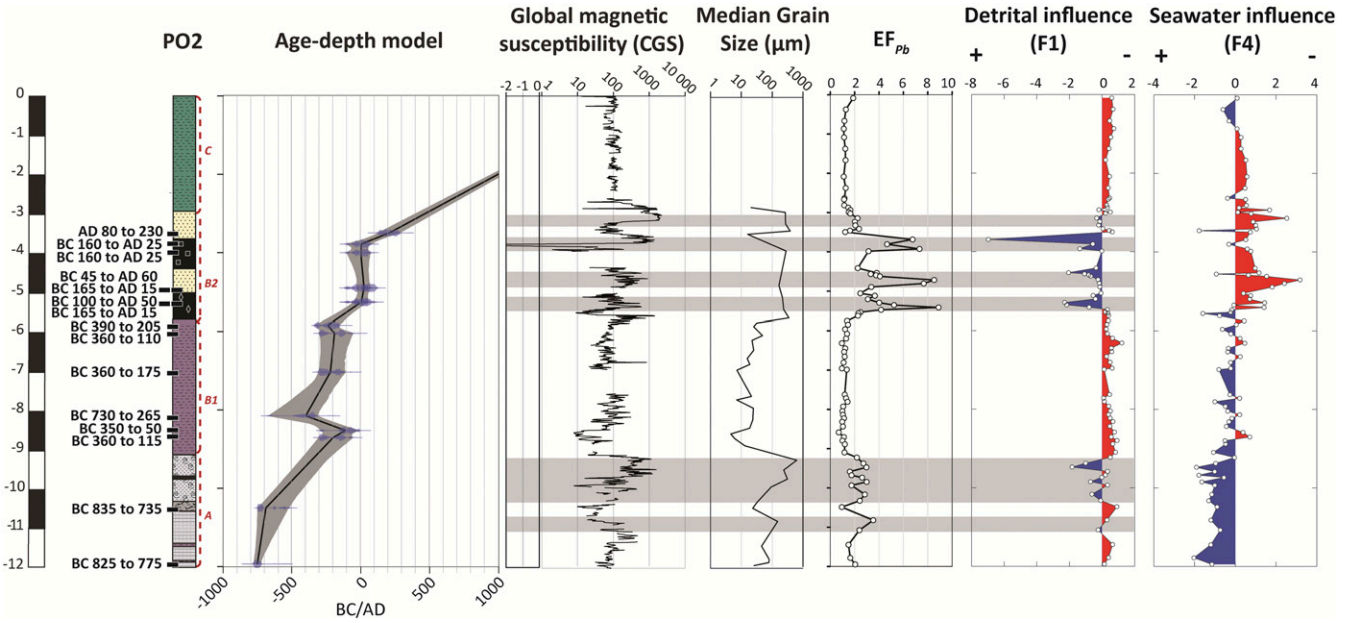

Fig. 1. Stratigraphic log of core PO2 showing the age-depth model of the core constructed using the Clam software (49) on 15 radiocarbon dates (shown with black labels on the stratigraphic log). Additional details on the age-depth model and the ^{14}C dates can be found in Fig. S4 and Table S1. The magnetic susceptibility values of the core along with the grain size 50 percentile (11), EF_{Pb}, and F1 (detrital influence) and F4 (seawater influence) of the factor analysis of major and trace element concentrations (the detailed distribution of the individual elements is shown in Fig. S2) are shown on the right-hand side. The gray shadings highlight the synchronicity between the highest EF_{Pb} values, detrital activity in the harbor basin (negative values of F1), the grain size 50 percentile, and magnetic susceptibility [centimeter, gram, second (CGS)].

of the second century BC. (*iii*) Subunit B2 forms the upper harbor sequence and contains levels of yellow sands brought in by repetitive floods of the Tiber, which occurred from the second century BC to the third century AD according to the ^{14}C age-depth model (Fig. 1). (*iv*) Unit C's yellow bedded silts from the third century AD onward represent floodplain deposits.

Elemental Concentrations. The lowest Pb values are consistent with the natural Pb background level of 22 ppm of the Tiber delta sediments (13, 14). The Pb enrichment factor (EF_{Pb}) records the relative enrichment of Pb relative to the natural environment (EF_{Pb} = 1 signifies no Pb excess). The evolution of EF_{Pb} in the harbor deposits (Fig. 1) goes from (*i*) values slightly above the natural Pb background level at the base of the stratigraphic section in the preharbor unit A located between 12- and 9-m core depth, with a mean EF_{Pb} of ∼2.2, to (*ii*) values highly above the natural Pb background in the harbor subunit B2 (between ∼6- and 3-m core depth; mean EF_{Pb} ∼ 3.8), with three peaks reaching EF_{Pb} values up to 9.

The stratigraphic record of Pb concentrations varies in concert with the presence of detrital material, magnetic susceptibility, and to a lesser extent, the median grain size (Fig. 1). The EF_{Pb} peaks in subunit B2 attest to a high-energy regime of fluvial activity (gray shadings in Fig. 1). Factor analysis of major and trace element abundances clearly identifies the siliciclastic component with terrigenous elements, such as the rare earth elements, K, Mn, and Ba, as the first factor (F1) (Fig. 1, Fig. S2, and Table S2). Lead concentrations of the bulk sediment are tightly associated with F1 (Fig. 1) (r = −0.66 between EF_{Pb} and F1), which emphasizes that the terrigenous fraction is the main carrier of this element. Factor 4 (F4) inferred from the factor analysis opposes Na to heavy metals, such as Pb, Sn, and Cd (Fig. 1, Fig. S2, and Table S2). The strong influence of Na within the stratigraphy reflects either the salinity of the harbor itself or the invasion of the sediments by the salt wedge. They are negatively correlated with the proportion of anthropogenic material carried by the Tiber. For both the Trajanic and Ostia harbors, the association of the ostracodal marine group with high sediment Na contents is clear evidence of a marine-dominated environment (11, 14, 15).

Lead Isotope Compositions. The labile Pb can be broken down into three well-defined components. In Fig. 2, the $^{204}Pb/^{206}Pb$ vs. $^{208}Pb/^{206}Pb$ vs. $^{207}Pb/^{206}Pb$ 3D plot shows an apparently ternary mixture between geologically "recent" Pb (components α′ and α″) and "old" Pb (component β). The recent natural Pb is a mixture of volcanic Pb from the Alban Hills (component α′) and sedimentary Pb from the Mediterranean outflow water (component α″ present in local carbonate sediments) well-separated by different $^{208}Pb/^{206}Pb$ values (2). The exact isotope compositions of the natural components α′ and α″ (Table S3) are somewhat arbitrary, but their specific assignment does not affect the conclusions reached about the order of magnitude and relative variations of the anthropogenic component β (Table S3 lists the Pb isotope composition of β).

The anthropogenic origin of the old Pb that dominates subunit B2 (Figs. 3 and 4) can be shown by converting the Pb isotope compositions into Pb model ages T_{mod}, $^{238}U/^{204}Pb$ (μ), and $^{232}Th/^{238}U$ (κ) ratios (Table S3) using the equations given by Albarède et al. (16). The advantages of this representation over that based on raw Pb isotope ratios have been shown in a number of geological and (geo)archeological contexts (2–4, 16–19). In the present case, Peninsular Italy is a geologically young mountain range (T_{mod} < 30 Ma); the presence of Hercynian Pb (T_{mod} > 200 Ma) in Ostia sediments, therefore, unambiguously signals contamination of local waters by foreign Pb, likely lead artifacts (Figs. 2 and 3). Quantitative breakdown of Pb isotopes into natural and anthropogenic components as proposed by Delile et al. (2) essentially reproduces the contamination patterns visible in the T_{mod} record of Ostia.

To characterize the evolution of the anthropogenic Pb signal, we use another pollution index f_{β}, which is based on the proportion of the anthropogenic β component in the Ostia sediments (equation details are in *Materials and Methods*). Beyond

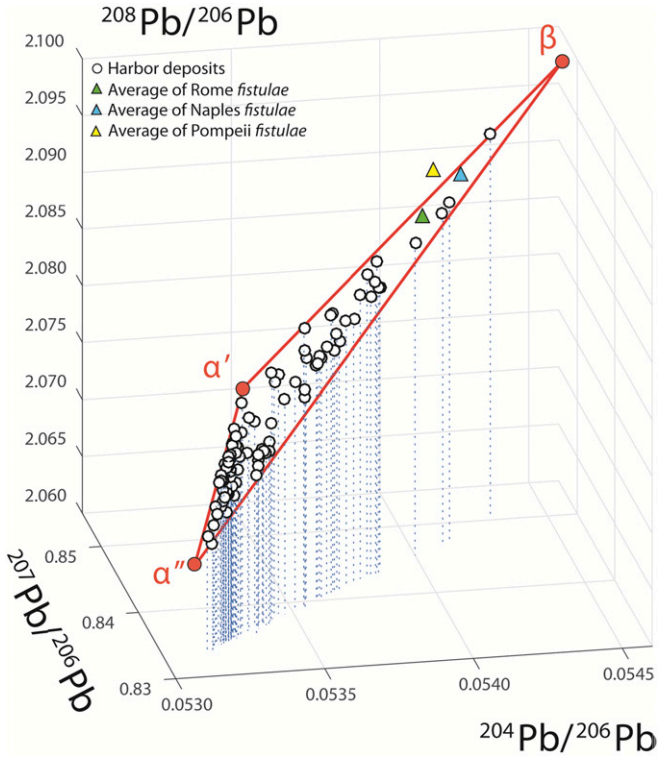

Fig. 2. 3D plot of $^{204}Pb/^{206}Pb$ vs. $^{208}Pb/^{206}Pb$ vs. $^{207}Pb/^{206}Pb$ measured on leachates from cores PO2 and PTXI-3. The track of the stippled blue drop lines suggests that the 3D dataset as a whole could be interpreted as a single alignment in $^{207}Pb/^{206}Pb$–$^{204}Pb/^{206}Pb$ space and therefore, as a two-component mixture. However, adding $^{208}Pb/^{206}Pb$ to the perspective shows that lead is a mixture of three separate components: α′, α″, and β. The three red lines connect components α′ and β, α″ and β, and α′ and α″. The α′ and α″ mixing line corresponds to unpolluted Tiber water and is composed of Mediterranean outflow water (α″) (50) and volcanic rocks from the Alban Hills (α′) (51, 52); β is the anthropogenic end member located near the *fistulae* from Rome (2), Naples (4), and Pompeii (26).

some minor trends, the EF_{Pb}, T_{mod}, f_β (Fig. 4), and raw Pb isotope ratio records (Fig. S3*A*) largely correlate, showing that the anthropogenic component does not fluctuate randomly but displays robust peaks and troughs.

Discussion

Natural and Anthropogenic Pb Sources. In Figs. 2 and 3, the pre-harbor and early harbor samples from Ostia (core PO2) and *Portus* (cores TR14, CN1, and PTXI-3) plot along the mixing line between the two local subcomponents α′ and α″. The sandy pre-harbor sediments (unit A of core PO2 and most of core PTXI-3) show consistently higher values of $^{208}Pb/^{206}Pb$ (Fig. S3*B*) and κ (Fig. 3) than the harbor sediments highly dominated by clays and silts (harbor subunit B1). This can be explained by changes in mineral sorting processes resulting from varying hydrodynamic levels. According to Garçon et al. (20), some heavy minerals concentrated in coarse sediments are extremely radiogenic, allowing sandy sediments to reach higher $^{208}Pb/^{206}Pb$ values (20) and thus, higher values of κ (r of $^{208}Pb/^{206}Pb$ vs. κ ∼ 0.7).

The intersection of two additional mixing lines—between α′ and α″ and the third anthropogenic component β—reveals that β is Hercynian in age (T_{mod} ∼ 325 Ma) (Fig. 3) and characterized by high $^{204}Pb/^{206}Pb$ (∼0.0546) (Fig. S3*B*). Sediments located on the mixing line α′-β correspond to Pb-contaminated particles that were transported in turbulent conditions, explaining their presence exclusively in the sandy subunit B2. In contrast, sediments falling along the α″-β trend were deposited under quieter hydrodynamic conditions, typically the silty floodplain deposits of unit C. Nevertheless, the whole of the *Portus* (cores TR14, CN1, and PTXI-3) and Ostia (core PO2) sediments (n = 177) affected by lead pollution converges toward the same distinct source, or mix of sources, of imported lead.

In Roman times, a substantial number of ships' hulls were sheathed with large millimeter-thick lead plates to protect their submerged portions against fouling and corrosion (21). Lead plates, anchors, and sounding lead weights are, however, unlikely to have been significant contributors to the anthropogenic Pb signal of Ostia sediments. The reasons for this are several. First, in seawater, lead passivation by the deposition of a film of chlorides and carbonates is fast and efficient (22). Second, because the earliest wreck with a hull sheathed in lead discovered so far dates to the midfourth century BC (23) and the practice had reached a peak by the end of the fourth century BC (21), if the sheathing of ship's hulls was a significant lead pollution source, we would expect an excess of lead to be recorded in the functional harbor unit B1, which covers the fourth and third centuries BC. Such lead pollution does not occur, however, until the harbor unit B2, which was deposited at the end of the use of the harbor (11, 15), from around the second century BC. In the same way, the practice of lead sheathing of ship's hulls was no longer significant from the middle of the first century AD (21), while Pb pollution of Rome's harbor water column lasts until the ninth century AD (2). Third, and most importantly, the anthropogenic component β is clearly homogenous (Figs. 2 and 3) (2). This is inconsistent with local contamination by vessels covered in lead plates of a variety of origins but consistent with distant sources well-mixed during the journey from Rome down the Tiber. Remarkably, the isotope abundances of component β match those of *fistulae* from the Roman urban water supply system (Figs. 2 and 3). The persistence of contamination for well over a millennium (200 BC to AD 800) and the uniqueness of its isotopic composition argue against random pollution. They rather suggest that a mechanism existed upstream from Ostia that efficiently mixed the isotopic compositions of all sources of anthropogenic Pb contributing to the anthropogenic signal so visible in the harbor sediments. Judging from the 20th century mean flow (230 m^3/s) (24), around 3% (7 m^3/s) of the Tiber's

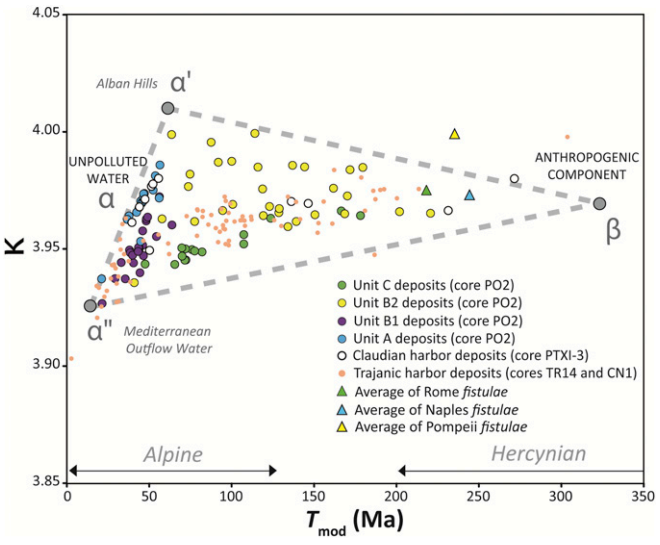

Fig. 3. Plot of T_{mod} vs. κ for leachates from cores PO2 (unit C in green, subunit B2 in yellow, subunit B1 in purple, and unit A in blue), PTXI-3 (Claudian harbor), TR14 (Trajanic harbor), and CN1 (*Canale Romano* deposits) and *fistulae* from Rome, Naples, and Pompeii (2, 4, 26) (the same plot for the raw Pb isotope ratios is in Fig. S3*B*).

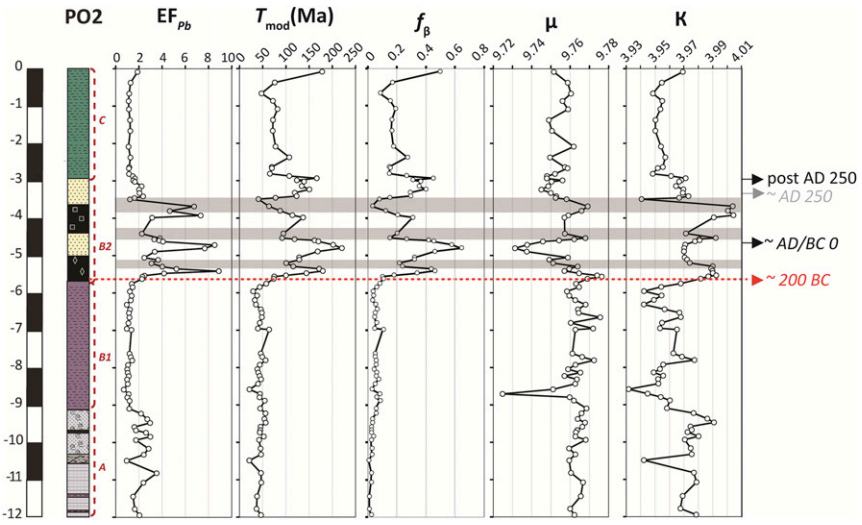

Fig. 4. Down core variations of EF_{Pb}, T_{mod}, f_β, μ, and κ. The red dotted line marks the first appearance of anthropogenic Pb pollution recorded in core PO2 from around 200 BC according to the age-depth model. The gray bands show the main declining trends of anthropogenic lead pollution discussed in this study (the same plot for the raw Pb isotope ratios is in Fig. S3*A*).

water was running through Rome's aqueducts at the peak of the Roman Empire (8, 25), a significant fraction of which passed through *fistulae*. Lead from Rome *fistulae*, therefore, seems the only acceptable source of contamination in Ostia sediments.

It is not clear whether the Pb ores derive from one or more mining districts, but recycling and salvaging practices of lead implemented by Romans (6, 10, 26) favor a mixture from several Hercynian sources (Germany, Spain, England, France). Such recycling would have contributed significantly to the stability of the isotopic signature of the imported Pb component over the long period observed. Additionally, the conspicuous isotopic stability, in turn, argues for long-term stability in the lead trade networks between Rome and the western half of its empire.

Control Factors of Pb Content. Changes in two main processes control the variation in the Pb contents of the PO2 core: (*i*) the input of Pb in the hydrological system upstream of the core and (*ii*) the transport of that Pb to the PO2 site. The major change in Pb inputs is the construction of the piped water distribution system in Rome. The imported Pb of Rome's pipes (with older Hercynian T_{mod} values) is progressively dissolved and transported down the Tiber to be deposited in the B2 and C units, except during disruptions to flow in the piped system occasioned by damage or neglect during political unrest, epidemics, natural disasters, etc. F1 and F4 correlate with two different transport processes: flooding by contaminated river water and dilution by uncontaminated seawater.

The correlation of EF_{Pb} with particle size as well as with the magnetic susceptibility and F1 shows that Pb excesses in the bulk sediment trapped in the harbor basin of Ostia were associated with Tiber flooding episodes that acted as a transport vector of Pb pollution. In other words, a period of increased river discharge (e.g., flooding) resulted in deposition of larger amounts of larger particles and hence, deposition of more Pb.

In subunit B2, imported Pb is present in the labile rather than the bulk fraction. It is correlated with F4 ($r = 0.6$) but not with F1 ($r = 0.09$). F4 is dominated by heavy metals, such as Sn and Cd, which, like T_{mod}, signal anthropogenic influence and which are opposed to Na (Fig. S2). Between 250 and 500 cm, several striking drops in Pb contamination levels occur ($^{206}Pb/^{207}Pb$ in Fig. S3*A*), which consistently are accompanied by steep marine (F4) peaks (Fig. 1). It, therefore, seems that sudden, uncontaminated seawater inputs into the harbor basin invariably resulted in a decrease in Pb pollution, probably because of a dilution effect. Dilution by an uncontaminated source of water is commonly observed in both ancient harbors [for example, Sidon (27)] and fluvial environments [such as the Ruhr River, a tributary to the Rhine (28), the Caima River (Portugal) (29), and the Belle Fourche River (United States) (30)].

A Chronology of Lead Pollution and Roman Urbanism. Fig. S4 reports errors on calendar ages from 200 BC to AD 300 using the values by Reimer et al. (31) and shows that ^{14}C chronology is particularly imprecise for the time interval covering the Roman Republic and Empire. For a given value of ^{14}C age, the range and, occasionally, the multiplicity of possible calendar ages in this interval are large, and uncertainties cannot be unambiguously represented by a single-error interval. Only those Pb isotope fluctuations that lasted in excess of age uncertainties are discussed here. With this caveat in mind, four main periods can nevertheless be distinguished from Fig. 4.

Uncontaminated environment (eighth/ninth to second century BC). From the bottom of the core to −563 cm (units A and B1), anthropogenic lead is not visible, even in harbor subunit B1, which dates from the foundation of Ostia in the fourth or early third century BC (32) to the beginning of the second century BC. Fig. 4 shows that contamination is not detected until the second century BC. This underscores once more that Pb pollution derives primarily from the dissolution of *fistulae* (Figs. 2 and 3). Lead *fistulae* would not be expected at Ostia in this period, since Ostia relied on wells for its water supply until the first half of the first century AD (33). The water of the Aqua Appia and Anio Vetus aqueducts at Rome, built in the late fourth century and early third century BC, respectively, were distributed by a lead-free system of masonry channels or terracotta or wooden pipes, of which only few have been found. It seems likely that these aqueducts supplied only a small number of focal points in the city, perhaps centrally located public fountains. Such a minimalist system was a far cry from that of Imperial Rome, which supplied hundreds of baths and private residences through a complex network of *fistulae* (10).

Manifestation of anthropogenic Pb (basal part of subunit B2). The next period (Fig. 4 and Fig. S3) is characterized by the first rise of anthropogenic Pb excesses in the sandy harbor subunit B2. The age-depth models of cores PO2 (Fig. 1) and PTXI-3 (Fig. S5 and

Table S1) both suggest that Pb contamination began around the second century BC.

The ^{14}C age-depth model receives some confirmation from scattered mentions in textual sources. The first dated stamps on lead pipes do not appear at Rome until 11 BC (10) and even later at Ostia (AD 37–41) (33–35). *Fistulae* seem to have been in use in water systems at the beginning of the first century BC in Rome (36), however, and by the late second century BC at nearby Alatri (10). Rome's system of public water basins and private connections was probably in operation by 184 BC, but lead pipes are not mentioned (9, 37). Already, Cato the Elder (234–149 BC) (38) used the word *fistula* as meaning "pipe."

The high-resolution Pb isotopic characterization of core PO2 provides continuous and detailed insight into water supply and urbanization upstream. After the first appearance of anthropogenic Pb in the harbor sediments of Ostia at −563 cm, the trends of decreasing $^{206}Pb/^{207}Pb$, $^{208}Pb/^{204}Pb$, $^{207}Pb/^{204}Pb$, $^{206}Pb/^{204}Pb$ (Fig. S3*A*), and μ (Fig. 4) with time as well as increasing EF_{Pb}, T_{mod}, and f_β (Fig. 4) argue for an overall increase of the imported Pb component. Like at other Roman cities (4, 34), this trend reflects the increase in the geographic extent and/or density of the lead pipe system as a result of urban development. At Rome, it is consistent with the repair and expansion of the water supply system that accompanied the commissioning of the Aqua Marcia (late 140s BC) and Aqua Tepula (125 BC) aqueducts (6).

Then, a sudden drop in EF_{Pb}, T_{mod}, and f_β and a sharp spike in $^{206}Pb/^{207}Pb$, $^{208}Pb/^{204}Pb$, $^{207}Pb/^{204}Pb$, $^{206}Pb/^{204}Pb$, and μ take place between −536- and −506-cm core depth (bottom gray bands in Fig. 4 and Fig. S3*A*), corresponding to the first century BC or early first century AD. After the Aqua Tepula, a century of rampant unrest and outright civil war prevented aqueduct construction and hampered maintenance (6). The Ostia PO2 core thus provides the first evidence of the scale of the contemporaneous reduction in flows in Rome's lead pipe distribution system—of the order of 50%—resulting in decreased inputs of lead-contaminated water into the Tiber. Octavian's (Augustus's) progressive defeat of his rivals during the 30s BC allowed his future son-in-law, Agrippa, to take control of Rome's water supply by 33 BC (6). Over the next 30 years, they repaired and extended the existing aqueduct and *fistulae* system as well as built an unprecedented three new aqueducts (6, 10), leading to renewed increase in Pb pollution of the Tiber river. This sequence of events is recorded as a sharp decrease in $^{206}Pb/^{207}Pb$, $^{208}Pb/^{204}Pb$, $^{207}Pb/^{204}Pb$, $^{206}Pb/^{204}Pb$ (Fig. S3*A*), and μ (Fig. 4) accompanied by a major spike in EF_{Pb}, T_{mod}, and f_β (Fig. 4) between −506- and −472-cm core depth. While the correlation between politics, stability, and lead isotopic composition is clear, the precise mechanism behind this correlation is undoubtedly complex and requires additional study.

Variability in pollution level (late first century BC/early first century AD to post-AD 250). The next chapter in the PO2 core stretches from −472 to −294 cm, covering the Roman Imperial period. The end of this phase falls outside the dated portion of the core. The overall trend shows continuing but declining Pb pollution from a peak around the beginning of this period. This continued Pb pollution is consistent with the Pb isotopic compositions of sediments deposited during the High Roman Empire in the Claudian (core PTXI-3) (Fig. S5) and Trajanic basins (core TR14) (2) at *Portus* as well as the canal leading to them (core CN1) (2), where T_{mod} values are ∼125–200 Ma and κ values are ∼3.96–3.98 (2), both indicative of imported lead. These sustained levels of anthropogenic Pb in multiple cores confirm the picture from textual and archeological data that the aqueduct and lead pipe distribution system was generally maintained until at least the midthird century AD (10, 39). Reduced dissolution of Pb because of insulation of the pipes by a coating of a limestone deposit known as travertine (8) is unlikely to be a factor in this decline. Coating of many ancient aqueducts, cisterns, fountains, and pools, including those at Rome and Pompeii, by centimeter-thick travertine deposits takes place as a result of carbon dioxide degassing and warming (40). Aqueducts, cisterns, fountains, and pools are well-ventilated, but in a pressurized piped system, like the ones that distributed water at Rome and Ostia, the water fills the entire pipe, inhibiting degassing and travertine deposition. Pipe damage—mentioned by two legal sources at Rome (6, 41)—probably led to regular replacement, thereby exposing fresh, uncoated lead for dissolution. The relative lack of travertine in pressurized pipes is borne out by our field observations at Rome (2) and around the Bay of Naples (42, 43), where almost all parts of the system are coated in travertine, except the pressurized pipes. Likewise, at Patara in Turkey (40), the pressurized inverted siphon pipes have much thinner travertine deposits than surrounding areas of the aqueduct. The travertine deposits from Pompeii (42) and the nymphaeum of Trajan at Ephesus (44) show elevated levels of lead that was clearly derived from the lead pipes and fittings, despite the widespread presence of travertine deposits in the systems. At Ostia, the situation is more complex: early lead contamination of travertine disappeared. The authors posit a change in water source (45).

The smooth declining trend in core PO2 is punctuated by two additional dips in Pb pollution, the second and third in the core (middle and top gray bands in Fig. 4 and Fig. S3*A*, respectively). The second decrease occurs from −470 to −440 cm (sometime between the late first century BC and the first century AD), and the third occurs from −370 to −350 cm (sometime from the first century to the early third century AD). Instability of the Tiber's flow regime is excluded as a cause for these drops because of the lack of correlation between f_β and F1 ($r = 0.2$ in subunit B2). These decreases coincide with two strong marine (F4) peaks (Fig. 1), suggesting that the most likely cause is the diversion of the contaminated Tiber water away from Ostia's harbor. Man-made links between the Tiber and the sea upstream of Ostia were constructed in this period: the northern canal, the *Canale Romano*, and the Claudian basin at *Portus* (midfirst century AD) followed by the Trajanic basin and probably, the northeastern canal (early second century AD) (46). These reductions in Tiber outflow would have initially and mechanically (*i*) brought less anthropogenic Pb and (*ii*) allowed more uncontaminated seawater to enter the harbor of Ostia, diluting the reduced Tiber-derived Pb. This would also explain why clear evidence of these anthropogenic Pb drops is not seen in the TR14 and CN1 cores (2). We cannot rule out, however, that the second and third drops in Pb pollution may be caused by damage or neglect of the water distribution system.

After the second drop (−470 to −440 cm), the renewed rise in Pb excesses shows that the Pb concentration in the water recovered to a level only slightly below the previous peak, while the values of f_β recovered to levels consistent with imported lead being the source (Fig. 4). After the third drop passed (∼−350 cm), the lead pollution in the harbor water column returned to approximately two-thirds ($f_\beta \sim 0.3$–0.5) (Fig. 4) of that of the major spike, with a surge of older Pb in leachates (∼125–175 Ma) and a dramatic drop in the $^{206}Pb/^{207}Pb$, $^{208}Pb/^{204}Pb$, $^{207}Pb/^{204}Pb$, $^{206}Pb/^{204}Pb$ (Fig. S3*A*), and μ (Fig. 4) derived from leaching of the *fistulae*. This last and durable Pb pollution phase recorded in the upper part of the PO2 core shows that maintenance of a somewhat reduced water system continued.

Decrease of the pollution level (post-AD 250). The last period, post-dating AD 250, is characterized by a decrease in imported lead ($f_\beta \sim 0.2$ in unit C) (Fig. 4). This decrease is also observed at the same time in the TR14 and CN1 cores at *Portus* (2) and is not associated with a strong period of marine influence (F4) (Fig. 1). It thus represents a contraction of the effective water distribution system at Rome, likely related to the increase in instability beginning in the third century AD. Indeed, after the midthird

century AD, no more aqueducts were built, and maintenance was on a smaller scale, while no pipe stamps can be dated to the period from the midthird to midfourth century AD (10). This period of receding Pb contamination corresponds to the apparent decline of Pb and Ag mining (47) and of overall economic activity in the Roman Empire (48).

Materials and Methods

Major and trace element concentrations were determined by complete digestion of the bulk sediment, whereas Pb isotope compositions were measured only on the most labile fraction to emphasize the anthropogenic contribution. A large selection of major and trace element concentrations was measured for the 12-m-long Ostia core PO2 every 14 cm (86 samples) (Dataset S1), while only Pb concentrations were analyzed for 12 samples from core PTXI-3. All samples from both cores were additionally measured for their Pb isotope compositions. *SI Text* has analytical details.

The proportion f_β of the β component in the leachate is calculated by least squares using three sets of equations: for example,

$$\left(\frac{^{204}Pb}{^{206}Pb}\right)_{\alpha' f\alpha'} + \left(\frac{^{204}Pb}{^{206}Pb}\right)_{\alpha'' f\alpha''} + \left(\frac{^{204}Pb}{^{206}Pb}\right)_{\beta f\beta} = \left(\frac{^{204}Pb}{^{206}Pb}\right)_{\text{leach}},$$

with similar equations for the $^{207}Pb/^{206}Pb$ and $^{208}Pb/^{206}Pb$ ratios. In these equations, f is the proportion of ^{206}Pb assigned to each component. A closure equation ensuring that all of the f values sum to one must be added.

ACKNOWLEDGMENTS. We thank three anonymous reviewers and the editor whose insightful comments helped improve the manuscript. We also thank the Soprintendenza Speciale per i Beni Archeologici di Roma e Sede di Ostia for the permission to drill core PO2 in the ancient harbor basin of Ostia and Philippe Telouk for ensuring that the mass spectrometers always worked. We acknowledge the ARTEMIS (Accélérateur pour la Recherche en sciences de la Terre, Environnement, Muséologie, Implanté à Saclay) program and radiocarbon laboratory of Lyon for carrying out the radiocarbon dating. Young Scientist Program of the Agence Nationale de la Recherche (CNRS) Grant ANR 2011 JSH3 002 01, Roman Mediterranean Ports Program European Research Council (ERC) Grant 339123, and the Ecole Française de Rome provided financial and logistic support.

1. Sherwin BD (2017) Pride and prejudice and administrative zombies: How economic woes, outdated environmental regulations, and state exceptionalism failed Flint, Michigan. *Univ Colo Law Rev* 88:653–720.
2. Delile H, Blichert-Toft J, Goiran J-P, Keay S, Albarède F (2014a) Lead in ancient Rome's city waters. *Proc Natl Acad Sci USA* 111:6594–6599.
3. Delile H, et al. (2015) Demise of a harbor: A geochemical chronicle from Ephesus. *J Archaeol Sci* 53:202–213.
4. Delile H, et al. (2016) A lead isotope perspective on urban development in ancient Naples. *Proc Natl Acad Sci USA* 113:6148–6153.
5. Nriagu JO (1983) *Lead and Lead Poisoning in Antiquity* (Wiley, New York).
6. Frontinus SI (2004) *De aquaeductu urbis Romae*, ed Rodgers RH (Cambridge Univ Press, Cambridge, UK).
7. Lewis M (1999) Vitruvius and Greek aqueducts. *Pap Br Sch Rome* 67:145–172.
8. Keenan-Jones D, Motta D, Garcia MH, Fouke BW (2015) Travertine-based estimates of the amount of water supplied by ancient Rome's Anio Novus aqueduct. *J Archaeol Sci Rep* 3:1–10.
9. Titus Livius (1835) *Histoire romaine de Tite Live* (C.L.F. Panckoucke, Paris).
10. Bruun C (1991) *The Water Supply of Ancient Rome: A Study of Roman Imperial Administration* (Finnish Society of Sciences and Letters, Helsinki).
11. Goiran J-P, et al. (2014) Geoarchaeology confirms location of the ancient harbour basin of Ostia (Italy). *J Archaeol Sci* 41:389–398.
12. Goiran J-P, et al. (2017) High chrono-stratigraphal resolution of the harbour sequence of Ostia: Palaeo-depth of the bassin, ship drought & dredging. *J Archaeol Suppl* 104:67–83.
13. Delile H (2014) Signatures des paléo-pollutions et des paléoenvironnements dans les archives sédimentaires des ports antiques de Rome et d'Éphèse. PhD thesis (Université Lumière Lyon 2, Lyon, France).
14. Delile H, et al. (2014b) Geochemical investigation of a sediment core from the Trajan basin at Portus, the harbor of ancient Rome. *Quat Sci Rev* 87:34–45.
15. Sadori L, et al. (2016) Palynology and ostracodology at the Roman port of ancient Ostia (Rome, Italy). *Holocene* 26:1502–1512.
16. Albarède F, Desaulty A-M, Blichert-Toft J (2012) A geological perspective on the use of Pb isotopes in Archaeometry. *Archaeometry* 54:853–867.
17. Desaulty A-M, Telouk P, Albalat E, Albarède F (2011) Isotopic Ag-Cu-Pb record of silver circulation through 16th-18th century Spain. *Proc Natl Acad Sci USA* 108:9002–9007.
18. Bouchet RA, Blichert-Toft J, Reid MR, Levander A, Albarède F (2014) Similarities between the Th/U map of the western US crystalline basement and the seismic properties of the underlying lithosphere. *Earth Planet Sci Lett* 391:243–254.
19. Blichert-Toft J, et al. (2016) Large-scale tectonic cycles in Europe revealed by distinct Pb isotope provinces. *Geochem Geophys Geosyst* 17:3854–3864.
20. Garçon M, Chauvel C, France-Lanord C, Limonta M, Garzanti E (2014) Which minerals control the Nd–Hf–Sr–Pb isotopic compositions of river sediments? *Chem Geol* 364:42–55.
21. Kahanov Y (1999) *Some Aspects of Lead Sheathing in Ancient Ship Construction. Tropis V, Hellenic Institute for the Preservation of Nautical Tradition. (Tzalas, H., Nauplia*, Greece*)*, pp 219–224.
22. Beccaria AM, Mor ED, Bruno G, Poggi G (1982) Corrosion of Lead in Sea Water. *Br Corros J* 17:87–91.
23. Parker AJ (1992) *Ancient Shipwrecks of the Mediterranean & the Roman Provinces* (Tempus Reparatum, Oxford).
24. Millero FJ, Macchi G, Pettine M (1981) The speciation of ions in Tiber river estuary waters. *Estuar Coast Shelf Sci* 13:517–534.
25. Blackman DR (1978) The volume of water delivered by the four great aqueducts of Rome. *Pap Br Sch Rome* 46:52–72.
26. Boni M, Maio GD, Frei R, Villa IM (2000) Lead isotopic evidence for a mixed provenance for Roman water pipes from Pompeii. *Archaeometry* 42:201–208.
27. Le Roux G, Veron A, Morhange C (2003) Geochemical evidences of early anthropogenic activity in harbour sediments from Sidon. *Archaeol Hist Lebanon* 18:115–119.
28. Moore JW, Ramamoorthy S, Ballantyne EE (1984) *Heavy Metals in Natural Waters: Applied Monitoring and Impact Assessment* (Springer, New York).
29. Ferreira da Silva E, et al. (2009) Heavy metal pollution downstream the abandoned Coval da Mó mine (Portugal) and associated effects on epilithic diatom communities. *Sci Total Environ* 407:5620–5636.
30. Marron DC (1989) The transport of mine tailings as suspended sediments in the Belle Fourche River, west-central South Dakota, USA. *IAHS-AISH Publication* 184:19–26.
31. Reimer PJ, et al. (2013) IntCal13 and Marine13 radiocarbon age calibration curves 0–50,000 years cal BP. *Radiocarbon* 55:1869–1887.
32. Brandt JR (2002) Ostia and Ficana: Two tales of one city? *Mediterranean Archaeology* 15:23–39.
33. Bukowiecki E, Monteix N, Rousse C (2008) Ostia Antica: Entrepôts d'Ostie et de Portus. Les Grandi Horrea d'Ostie. *Mélanges de l'Ecole française de Rome - Antiquité* 120:211–216.
34. Bruun C (2002) L'amministrazione imperiale di Ostia e Portus. *Ostia e Portus nelle loro relazioni con Roma, Acta instituti romani finlandiae*, eds Bruun C, Gallina A (Institutum Romanum Finlandiae, Rome), pp 161–192.
35. Ricciardi MA, Scrinari VSM (1996) *La civiltà dell'acqua in Ostia antiqua* (Fratelli Palombi, Rome).
36. Cicero (1856) *The Orations of Marcus Tullius Cicero* (H. G. Bohn, London).
37. Plutarch (1914) Marcus Cato. *The Parallel Lives* (Loeb Classical Library, Harvard Univ Press, Cambridge, MA), Vol II.
38. Cato MP (1934) *On Agriculture* (Loeb Classical Library, Harvard Univ Press, Cambridge, MA).
39. Ashby T (1935) *The Aqueducts of Ancient Rome*, ed Richmond I (Oxford Univ Press, Oxford).
40. Sürmelihindi G, Passchier CW, Baykan ON, Spötl C, Kessener P (2013) Environmental and depositional controls on laminated freshwater carbonates: An example from the Roman aqueduct of Patara, Turkey. *Palaeogeogr Palaeoclimatol Palaeoecol* 386:321–335.
41. Pharr C, Davidson TS, Pharr MB (1952) *The Theodosian Code and Novels and the Sirmondian Constitutions* (Princeton Univ Press, Princeton).
42. Keenan-Jones D, Hellstrom J, Drysdale R (2011) Lead contamination in the drinking water of Pompeii. *Pompeii: Art, Industry and Infrastructure*, eds Poehler E, Flohr M, Cole K (Oxbow Books, Oxford), pp 131–148.
43. Keenan-Jones D (2010) The Aqua Augusta Regional water supply in Roman and late antique Campania. PhD dissertation (Macquarie University, Sydney).
44. Prochaska W, Quatember U (2006) The analysis of sinter samples and hydraulic mortars from the Nymphaeum Traiani at Ephesus. *Cura Aquarum in Ephesus*, ed Wiplinger G (Ephesus, Selçuk, Turkey), pp 509–514.
45. Carlut J, Chazot G, Dessales H, Letellier É (2009) Trace element variations in an archeological carbonate deposit from the antique city of Ostia: Environmental and archeological implications. *C R Geosci* 341:10–20.
46. Salomon F, et al. (2014) A harbour–canal at Portus: A geoarchaeological approach to the Canale Romano: Tiber delta, Italy. *Water Hist* 6:31–49.
47. Kylander M, et al. (2005) Refining the pre-industrial atmospheric Pb isotope evolution curve in Europe using an 8000 year old peat core from NW Spain. *Earth Planet Sci Lett* 240:467–485.
48. Scheidel W (2009) In search of Roman economic growth. *J Roman Archaeol* 22:46–70.
49. Blaauw M (2010) Methods and code for "classical" age-modelling of radiocarbon sequences. *Quat Geochronol* 5:512–518.
50. Stumpf R, Frank M, Schönfeld J, Haley BA (2010) Late Quaternary variability of Mediterranean Outflow Water from radiogenic Nd and Pb isotopes. *Quat Sci Rev* 29: 2462–2472.
51. Conticelli S, D'Antonio M, Pinarelli L, Civetta L (2002) Source contamination and mantle heterogeneity in the genesis of Italian potassic and ultrapotassic volcanic rocks: Sr–Nd–Pb isotope data from Roman Province and Southern Tuscany. *Mineral Petrol* 74:189–222.
52. D'Antonio M, Tilton GR, Civetta L (1996) Petrogenesis of Italian alkaline lavas deduced from Pb-Sr-Nd isotope relationships. *Earth Processes: Reading the Isotopic Code*, Geophysical Monographs, eds Basu A, Hart S (American Geophysical Union, Washington, DC), pp 253–267.
53. White WM, Albarède F, Télouk P (2000) High-precision analysis of Pb isotope ratios by multi-collector ICP-MS. *Chem Geol* 167:257–270.
54. Albarède F, et al. (2004) Precise and accurate isotopic measurements using multiple-collector ICPMS. *Geochim Cosmochim Acta* 68:2725–2744.
55. Eisele J, Abouchami W, Galer SJG, Hofmann AW (2003) The 320 kyr Pb isotope evolution of Mauna Kea lavas recorded in the HSDP-2 drill core. *Geochem Geophys Geosyst* 4:1–32.
56. Blaauw M, Christen JA (2011) Flexible paleoclimate age-depth models using an autoregressive gamma process. *Bayesian Anal* 6:457–474.